STABILITY STUDY OF CRREL PERMAFROST TUNNEL

By Scott Lin Huang,[1] Nolan B. Aughenbaugh,[2] M. ASCE, and Ming-Chee Wu,[3] S. M. ASCE

ABSTRACT: Underground excavated openings in permafrost can have significant ground stability problems if the thermal regime of the area is disturbed. Other factors influencing ground stability besides temperature variation include dimensions of the excavation, thickness of the overburden, and geometry of the opening. This paper summarizes the results of a research project conducted at the U.S. Army Cold Regions Research and Engineering Laboratory (CRREL) permafrost tunnel. The relationships between the ground temperature, the roof span dimensions, and the vertical convergence rate of the CRREL tunnel correlates with a combined exponential and logarithmic model. The continuous deformation of the tunnel is primarily temperature dependent. In addition to the effect of temperature, the opening width also exhibits a strong influence on tunnel deformation. The span length gradually achieved a constant effect upon tunnel deformation as the opening width increased. The overburden thickness also exhibits an influence on convergence rate.

INTRODUCTION

Because of its isolated geographic location and severe climatic conditions, Alaska, the largest state in the United States, is very sparsely populated and relatively undeveloped. Expansion of the state's economic base and associated civil works has been, and will continue to be dependent mostly upon the exploitation of its abundant mineral resources. Production from the Prudhoe Bay oil field, via the 800 mile-long Alaska pipeline to an ice free port in Valdez, has been the single most important economic base for Alaska's recent population growth and multiple civil works projects. Mining promises to add a similar input in the future. However, due to the fact that most of Alaska lies in arctic and subarctic climatic zones, normal engineering construction and mining practices are complicated by severe weather and permafrost.

Over 80% of the land in Alaska is underlain with permafrost, Fig. 1. Permafrost, or perennially frozen ground, is defined as earth material that has been in a frozen state for at least two consecutive years. The permafrost regions of Alaska are divided into two zones according to the occurrence of thawed ground. The continuous zone, in the north, is totally underlain by permafrost except for areas concomitant with large water bodies. The discontinuous zone, situated in southern Alaska, is characterized by permafrost and thawed ground existing together. Typically, the thawed soil and rock are situated on south-facing slopes and in well-drained areas. The north-facing slopes and valley bottoms are

[1]Asst. Prof., Dept. of Mining and Geological Engrg., Univ. of Alaska, Fairbanks, AK 99775-1190.

[2]Prof., Dept. of Geology and Geological Engrg., Univ. of Mississippi, University, MS 38677.

[3]Grad. Student, Dept. of Geological Engrg., Univ. of Missouri, Rolla, MO 65401.

Note.—Discussion open until January 1, 1987. To extend the closing date one month, a written request must be filed with the ASCE Manager of Journals. The manuscript for this paper was submitted for review and possible publication on November 11, 1985. This paper is part of the *Journal of Geotechnical Engineering*, Vol. 112, No. 8, August, 1986. ©ASCE, ISSN 0733-9410/86/0008-0777/$01.00. Paper No. 20831.

J. Geotech. Engrg., 1986, 112(8): 777-790

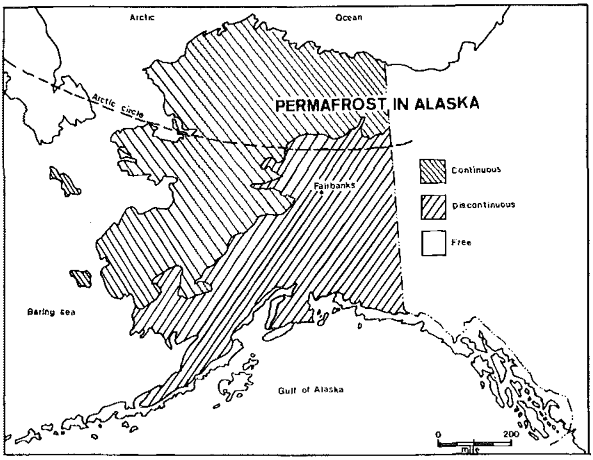

FIG. 1.—Distribution of Permafrost in Alaska (after Hartman and Johnson, 1978)

generally frozen. Fine-grained sediments and muskeg deposits are consistently frozen and thaw bulbs may occur under rivers and lakes.

Soil and rock mechanics analysis and design must take into consideration the properties of permafrost and the behavior of the frozen earth materials. Also, much consideration must be given to the drastic changes that can occur in these materials if the temperature conditions change.

The features of permafrost that influence or control engineering properties of the soils include the active layer, which thaws during the summer and freezes again in the winter, ice lenses, ice wedges, and ice-rich ground, in which the volume of ice exceeds the void volume of the thawed soil. Potentially detrimental permafrost is generally confined to fine-grained, ice-rich deposits.

The central interior of Alaska around Fairbanks is known for its rich and abundant placer deposits of gold. This region also is blanketed with thick loess and ice-rich deposits that overlie gravels containing placer gold. In early gold mining operations, miners sank shafts through the silt to get to the gold bearing gravels. Later, mining companies used various techniques to thaw and wash away the silt prior to dredging the center of the placer stream valleys. They left considerable amounts of gold near the valley walls and adjoining tributary streams. More recently, miners have used construction excavation equipment to placer mine the gold. Sluicing the silt downstream, however, is no longer permitted and meeting stream-water quality standards could severely reduce, if not completely shut down, this mining method.

With the possible termination of present placer mining methods, much interest has been shown in tunneling through the silt to mine the gold-rich gravel. In addition, tunnels and permanent excavations in these thick surficial deposits for construction and civil works has brought attention to the need to investigate the stability of openings in frozen, ice-rich silt.

Underground excavation in permafrost can have significant ground stability problems if the thermal regime of the area is disturbed (4). Other

J. Geotech. Engrg., 1986, 112(8): 777-790

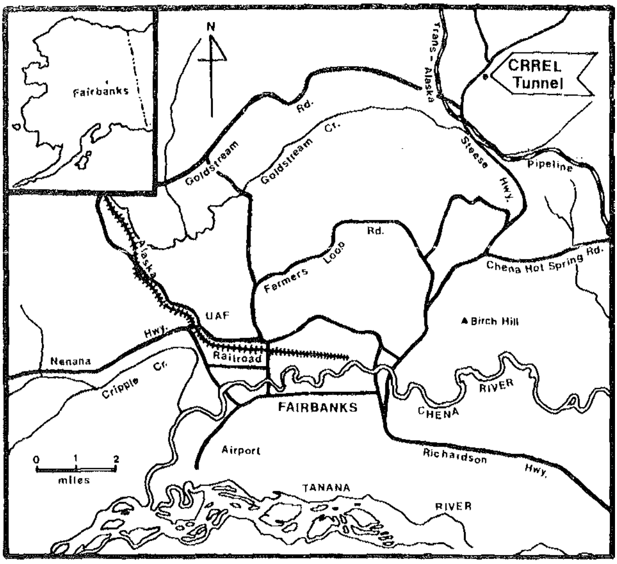

FIG. 2.—Location of the USA CRREL Permafrost Tunnel (after Péwé, 1958)

factors influencing ground stability besides temperature variation are dimensions of the opening, thickness of the overburden (3), ventilation, humidity level, and geometry of the tunnel system.

Because of the dominance of frozen silt in interior Alaska and because of frequent excavation activities in this surficial deposit, the authors conducted a study to investigate ground stability problems related to underground excavation in frozen silt. In order to obtain the necessary information for a practical design, the U.S. Army Cold Regions Research and Engineering Laboratory (CRREL) permafrost tunnel was used for the investigation.

The CRREL permafrost tunnel is located approximately 12 miles north of Fairbanks, Fig. 2, and presently is the only active research tunnel in perennially frozen ground in the western world. Due to the uniqueness of the tunnel, there have been a series of research projects carried out by the writers and other investigators since the tunnel's inception in 1963 (2–5,8). This paper focuses mainly on the effects of ground temperature and the unsupported roof span on the deformation of the tunnel. The influence of the opening width of an underground thickness excavation on the roof stability is one of the most important aspects of underground construction problems in arctic regions. In addition to insitu temperature conditions and roof span, the variations of tunnel closure due to the changes of overburden also will be discussed.

Geologic Setting

Fairbanks, physiographically, is near the southern limit of the Yukon-Tanana Upland of interior Alaska. The Yukon-Tanana Upland consists

J. Geotech. Engrg., 1986, 112(8): 777-790

mainly of rolling bedrock hills covered with loess. The valleys are filled with secondarily deposited silt. Gold mining operations in the vicinty of the study site began in 1929 by placer dredging. This dredging formed the nearly vertical escarpment on the hillside in which the CRREL permafrost tunnel was excavated.

The geology of the Fairbanks area, as well as most of interior Alaska, has been documented by Péwé (6). The bedrock in this area consists primarily of Birch Creek schist of Precambrian to Paleozoic age. It is a gray to brownish graphite-quartz-calcite schist or quartz-mica schist. The schist has been intruded by pegmatites, granite, and quartz diorites of Mesozoic age.

The top of schist bedrock is highly weathered and is covered by ice-cemented silts and gravels. The older gold bearing gravels are confined to the stream valleys and are capped by thick silt sections. Silt also mantles the hills.

The CRREL Tunnel

Excavation of the CRREL tunnel began in the winter of 1963. The purpose was to evaluate the performance of excavation techniques in frozen silt. Its portal was cut into a nearly vertical silt escarpment formed by old placer mining operations at the margin of the Glenn Creek valley. During the following three winters the tunnel was extended through the frozen silt to a maximum length of 109.7 m (360 ft). A vertical shaft, 13.7 m (45 ft) in length, was drilled during the winter of 1966 for ventilation purposes.

Through the winter of 1968–69, the U.S. Bureau of Mines drove a winze starting at an existing sideroom 30.5 m (100 ft) from the portal. The decline slope was approximately 12 degrees. This excavation passed through the gold-bearing frozen gravels into the weathered schist bed-

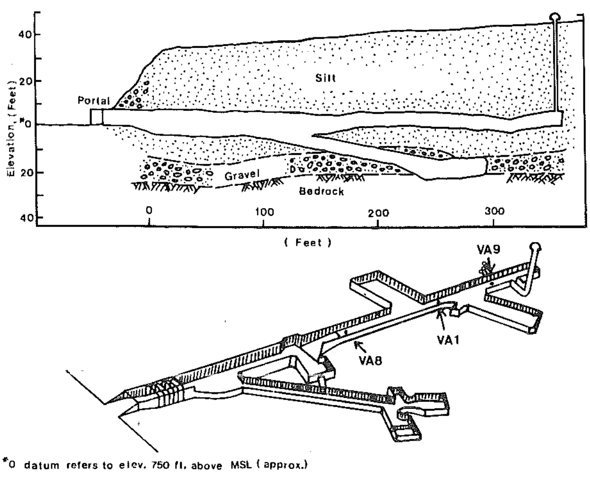

FIG. 3.—Idealized Geological Cross Section of Tunnel and Location of Monitoring Devices (after Thompson and Sayles, 1972)

rock in order to evaluate the possibility of underground mining of deep placers in permafrost areas.

Fig. 3 shows an idealized cross section of the tunnel. According to a geological study conducted by Sellmann (7), the gravels, interbedded by sand and silt layers, are stream deposited. The excavation reveals a typical stratigraphic sequence of frozen sediments and permafrost features for this area. The tunnel and its chambers are accessible and well maintained in a frozen state by the circulation of cold outside air during the winter and by a refrigeration system in the summer. The tunnel provides a unique opportunity for investigating the engineering properties of permafrost.

Engineering Properties

The silt sections at the studied site attain a maximum thickness of 16.8 m (55 ft). Analyses by Huang (2) of silt samples from the tunnel indicate that 68% of the material is within the silt size range. The uniformity coefficient is approximately 3.8 which indicates that the material is fairly uniform in size.

The bulk unit weight of the silt varies from 1,425.6 kg/m^3 (89 pcf) to 2,082.3 kg/m^3 (130 pcf). The moisture content fluctuates from 32–139%. The dry unit weight varies from a low of 624.7 kg/m^3 (39 pcf) to 1,393.6 kg/m^3 (87 pcf) and averages 865.0 kg/m^3 (54 pcf). The void ratio and porosity of the silt average 2.3 and 31%, respectively. Exposures of the silt in the tunnel contain massive ice-wedges, small ice-lenses, and large, clear ice masses in addition to intergranular cementing ice. The large volume of ground ice, 53–80% by volume, causes unusual engineering problems. The strength of the frozen silt is strongly influenced by the high ice volume.

The average thickness of the gold-bearing gravel in the vicinity of the tunnel is about 4.0 m (13 ft). Moisture content of the gravel varies from 8.9–10.3%. Particle size analyses revealed that 55% of the deposit is in the gravel size range. The uniformity coefficient is approximately 4.5 which indicates that the gravel deposit is not well sorted. Like the silt, the gravel is bonded with ice. Ice is visible in the voids but the gravel appears to retain much particle-to-particle contact. In general, the gravel is much more stable than the silt and the strength of the frozen gravel is strongly affected by temperature and ice content. At the temperature conditions in the tunnel, the uniaxial compressive strength of the gravel is about 20.7 MPa (3,000 psi) at a loading rate of 12.8 microstrain/sec. The unified soil classification system groups this gravel as GP-GW material.

The top portion of the schist bedrock is highly altered and forms a clay layer. The dry unit weight of this material is 2,018.3 kg/m^3 (126 pcf) and the moisture content is from 6.5–19.9%. The Liquid Limit and the Plasticity Index of the weathered schist average 19% and 4%, respectively (5). The altered rock is classified as GW-GM soil.

Field Studies

The CRREL tunnel was instrumented with a dozen vertical convergence/temperature monitoring stations, Fig. 3, to measure convergence

J. Geotech. Engrg., 1986, 112(8): 777-790

and temperature variations in the tunnel. In addition to the temperature and convergence monitoring stations, three hydraulic borehole load cells were installed in the sidewall of the tunnel near station VA9. The load cells were installed to record any possible convergence-induced stress within the wall of the tunnel.

The vertical convergence stations consisted of machine bolts anchored to the roof and floor. The bolts had an eye ring at one end and a threaded shell at the other end. The shells spread outward when the bolts were tightened. The roof anchors were inserted into the silt to a depth of about 10.2 cm (4 in.). The floor anchors, with steel extensions, were inserted about 20.3 cm (8 in.) into the floor. Both the roof and floor anchors were grouted with a slurry to prevent the bolts from loosening. The slurry was a mixture of sublimated silt and water with a volumetric ratio of 3:1. The floor anchors were placed about 5.1 cm (2 in.) below the ground surface and capped with a piece of plywood in order to avoid any accidental disturbance. Water mist was sprayed around the anchors once every two weeks to reduce sloughing of frozen silt caused by sublimation of ice within the grout materials.

The height variations between the roof and floor anchors were measured by a tape extensometer. A provision for insuring the same tension during each measurement produced relatively accurate readings. Measurements were read from a dial gage with 0.0254 mm (0.001 in.) divisions.

A string of thermistors was installed adjacent to each roof anchor to measure ground and air temperatures. Each string contained two thermistor crystals; one inserted to a depth of 0.3 m (1 ft) in the roof and the other placed on the surface of the roof. For protection purposes, the thermistors were placed in small glass bottles filled with epoxy before insertion into the hole. The hole was later grouted with the same slurry as that used in the installation of the vertical convergence stations. Temperature variations sensed by the thermistors were recorded by a portable, digital multimeter with an accuracy of 0.06° C (0.1° F).

Three pressure cells were installed as a set into the sidewall of the tunnel in an attempt to determine the variation in stress from the tunnel surface inward. Also, monitoring of the cells would indicate any changes in the stress conditions with time as the tunnel deformed. The three cells were implanted at depths of 20.3 cm (8 in.), 35.6 cm (14 in.), and 55.9 cm (22 in.) as shown in Fig. 3. The cells measured only vertical stresses.

Results

The air temperature was found to fluctuate in response to the air flow from ventilation. When the fan was off and circulation ceased, the stagnant air became temperature stratified. Fig. 4 shows the variation of air temperature at station VA9 during the monitoring period. The in-situ silt temperature was recorded at a depth of 0.3 m (1 ft) into the roof stratum. The 0.3 m (1 ft) reference temperature proposed by Huang and Garbeil (4) provides an indication of the temperature variation through time. Fig. 4 also indicates the ground temperature readings from station VA9.

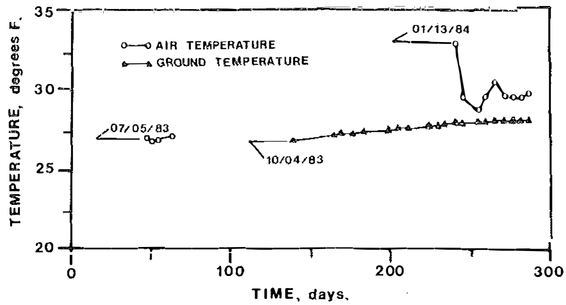

FIG. 4.—Measurements of Ground and Air Temperatures at Station VA9

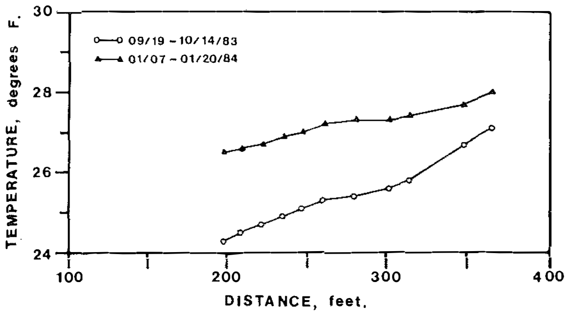

FIG. 5.—Ground Temperature Distribution along Tunnel

Both the ground and air temperatures exhibited an increasing trend during the winter months. This trend was attributed to the discontinuous use of the refrigeration system during the winter and the stagnant condition of air. It is interesting to note that the air temperature was approximately 0.8° C (1.5° F) higher than the ground temperature. This reversal was not expected prior to this study. Fig. 5 shows the ground temperature profiles of the tunnel for both the summer and winter seasons. The curves show a trend in which the temperature increases as it progresses from the portal towards the end of the tunnel. This phenomenon indicates a very low air-flow velocity inside the tunnel and a stagnant condition near the end of the tunnel. During the winter months, when the portal doors were open, the very cold outside air migrated slowly into the tunnel by gravity flow. In contrast, in the summer, the tunnel's entrance doors were closed and the cooling system was turned on. The cold air blown from the refrigeration system lowered the ground temperature of the tunnel by 0.6–1.1° C (1–2° F).

Convergence data at station VA9 are plotted in Fig. 6. It can be seen on the two graphs, and when compared with the data in Fig. 4, that the higher convergence rate corresponds to the higher ground temperature. The convergence rates of the tunnel were analyzed by dividing the measurements on a two week basis as listed in Table 1. The corresponding ground temperature was estimated by averaging the thermistor readings

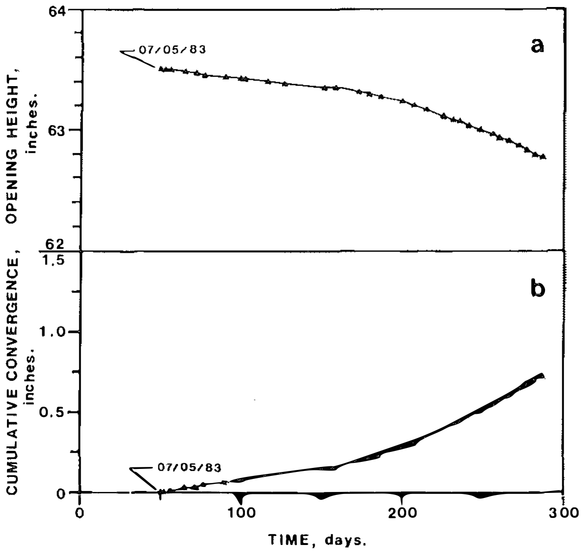

FIG. 6.—(*a*) Variation of Opening Height; (*b*) Cumulative Convergence at Station VA9

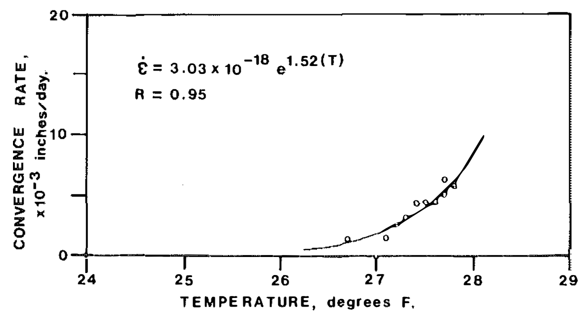

FIG. 7.—Relationship between Convergence Rate and Ground Temperature at Station VA9 (Correlation Coefficient = 0.95)

for a depth of 0.3 m (1 ft) during the same period. The vertical convergence rate versus ground temperature at station VA9 is plotted in Fig. 7. An exponential equation was proposed by Huang (2) to quantify the relationship between the temperature and the creep deformation rate of a gravel room in permafrost. The authors used the same approach and verified the effect of temperature on the convergence rate of frozen silt opening. The general formula of the relationship between convergence rate ($\dot{\epsilon}$) and temperature (T) can be expressed as follows:

$$\dot{\epsilon} = ae^{b(T)} \quad (1)$$

The coefficients, a and b, and the Correlation Coefficient of each model are listed in Table 2.

TABLE 1.—Summary of Biweekly Convergence Rate and Site Information

Item (1)	VA (2)	VA1 (3)	VA2 (4)	VA3 (5)	VA4 (6)	VA5 (7)	VA6 (8)	VA7 (9)	VA8 (10)	VA9 (11)	VA10 (12)	VA11 (13)	VA12 (14)
	Convergence Rate (× 10^{-3} in./day)												
09/19–10/14	1.68	1.08	1.40	0.48	0.36	0.12	0.08	0.16	0.20	1.32	2.36		—
10/14–11/04	2.18	1.90	2.89	1.11	0.43	0.36	0.15	0.54	0.75	1.47	2.61	—	—
11/04–11/18	3.43	3.57	5.14	1.79	0.79	0.86	0.50	—	0.07	2.57	3.72	3.29	3.36
11/18–12/03	3.29	3.29	5.71	2.64	1.29	0.07	0.36	—	0.07	3.14	5.00	4.86	3.71
12/03–12/16	4.25	4.16	5.89	2.56	1.77	1.23	0.46	1.15	0.21	4.27	4.94	5.23	4.59
12/16–12/28	3.27	3.00	4.45	1.64	1.18	0.73	0.73	1.00	0.18	4.36	3.64	3.64	4.55
12/28–01/07	4.67	5.29	9.04	1.75	0.92	1.00	2.21	1.59	2.00	4.46	5.29	4.46	6.71
01/07–01/18	4.40	4.75	10.40	5.27	1.70	1.95	0.49	1.72	0.15	5.02	5.63	6.36	5.18
01/18–02/01	5.07	6.75	11.19	5.75	3.50	1.38	2.75	2.32	1.63	6.25	7.00	7.19	7.38
02/01–02/13	6.58	7.00	13.25	5.75	2.83	1.67	0.59	1.67	1.08	5.75	5.92	7.84	9.42
02/13–02/28	5.13	7.47	12.40	6.40	2.73	3.00	2.47	2.33	1.53	6.00	6.67	7.87	8.87
Average	4.00	4.39	7.43	3.19	1.59	1.12	0.98	1.13	0.72	4.06	4.80	5.64	5.97
	(*a*) Initial Opening												
Height (ft)	5.52	4.56	4.54	5.33	5.67	5.74	5.96	5.79	6.11	5.26	5.17	5.31	5.33
Width (ft)	11.57	13.48	46.75	10.97	12.30	11.97	12.53	11.37	13.18	10.36	11.49	30.13	21.25
Overburden (ft)	41	41	40	38	38	38	38	37	35	41	41	42	43

By plotting the average convergence rate at each station with respect to the corresponding average ground temperature, Fig. 8, an exponential relationship is evident. Deviation from the average trend, however, is larger than the individual curve indicated in Fig. 7 and Table 2 especially at the higher convergence rates. Because of this relatively large deviation, other factors were considered to have had a certain degree of influence.

Among many other factors, the geometry was considered to have had the strongest influence on the convergence of the tunnel. Three elements were regarded as geometric factors: (1) The overburden thickness; (2) the average height of the tunnel; and (3) the width of the unsupported roof span. Table 1 also summarizes the value of the geometric

TABLE 2.—Statistical Analysis of Ground Temperature Effect

Station (1)	*a* (2)	*b* (3)	Correlation coefficient (4)
VA	1.865×10^{-9}	0.782	0.94
VA1	2.860×10^{-12}	1.038	0.95
VA2	6.489×10^{-13}	1.113	0.96
VA3	1.035×10^{-14}	1.237	0.92
VA4	3.201×10^{-13}	1.092	0.88
VA5	3.260×10^{-16}	1.337	0.72
VA6	9.030×10^{-17}	1.389	0.80
VA7	1.356×10^{-13}	1.136	0.99
VA8	1.530×10^{-9}	0.74	0.42
VA9	3.025×10^{-18}	1.517	0.95
VA10	4.862×10^{-13}	1.075	0.95
VA11	2.010×10^{-12}	1.046	0.85
VA12	2.084×10^{-15}	1.303	0.93

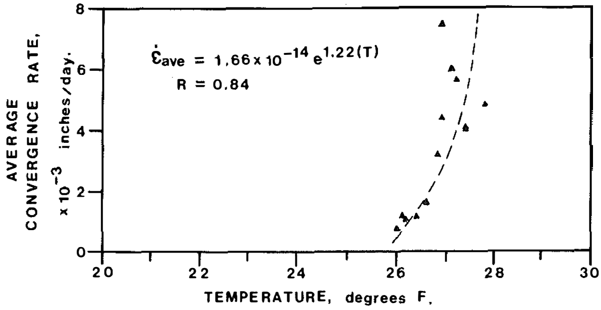

FIG. 8.—Average Convergence Rates of the Tunnel versus Average Ground Temperatures (Correlation Coefficient = 0.84)

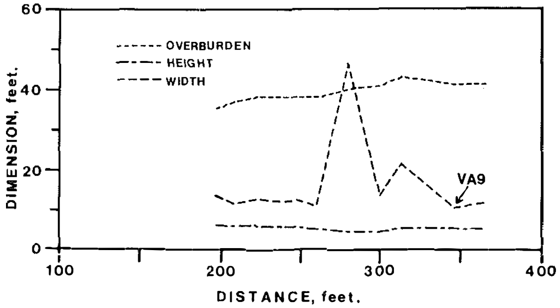

FIG. 9.—Distributions of Overburden Thickness, Opening Height and Width along Tunnel

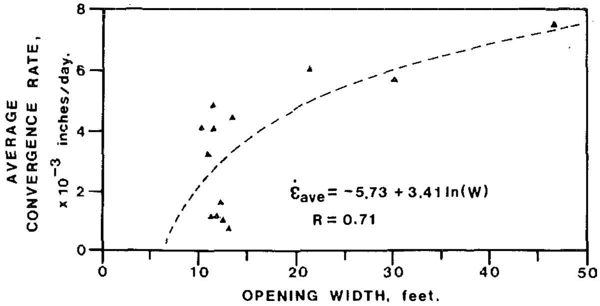

FIG. 10.—Average Convergence Rates of Tunnel versus Opening Widths (Correlation Coefficient = 0.71)

factors at each monitoring station. Fig. 9 shows these three elements along the tunnel. The analysis of the effect of tunnel width on the convergence rate was documented by comparing the average convergence rate of each station with the corresponding opening width. Fig. 10 provides convergence information without considering the temperature variation. An empirical curve fitting approach was performed to assess the effect. The regression curve with the correlation coefficient of 0.71 given in the diagram can be expressed by a logarithmic model of the average convergence rate in terms of the opening width (W):

$$\dot{\epsilon}_{ave}\ (\times 10^{-3}\ \text{in./day}) = -5.73 + 3.41 \ln (W) \quad (2)$$

A steep slope of the trend at shorter roof widths and a reduced slope toward larger widths indicate that change of average convergence rate is also opening width-dependent. As the opening width increases, the effect of tunnel deformation seems to achieve a condition under which a near constant convergence rate is maintained.

To combine the effects of temperature and tunnel width, ratios of the observed convergence rates of a given monitoring station and the convergence rates predicted by Eq. 2 were plotted against the corresponding ground temperature. Fig. 11 shows the relationship. The curve describes an exponential model with a correlation coefficient of 0.95 as follows:

$$\frac{\dot{\epsilon}}{\dot{\epsilon}_{ave}} = 2.54 \times 10^{-14}\, e^{1.15(T)} \quad (3)$$

Rearrangement of Eq. 3 brings the final equation into a form which

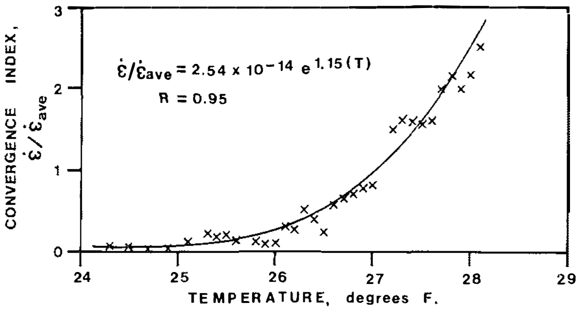

FIG. 11.—Relationship between Convergence Indices and Ground Temperatures (Correlation Coefficient = 0.95)

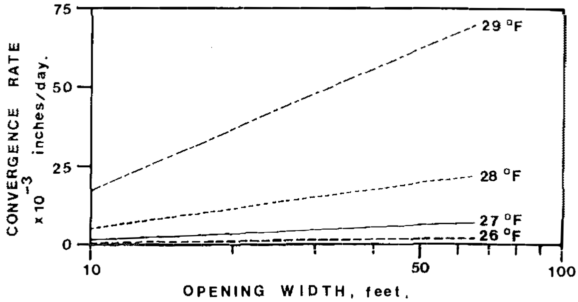

FIG. 12.—Plot of Eq. 4 Showing Relationship between Convergence Rate, Ground Temperature, and Opening Width

contains both ground temperature and tunnel width as independent factors.

$$\dot{\epsilon}\ (\times 10^{-3}\ \text{in./day}) = \{-5.73 + 3.41 \ln(W)\} \times \{2.54 \times 10^{-14} e^{1.15(t)}\} \quad \ldots\ldots (4)$$

An alternative and useful representation of the above equation is to plot the convergence rate versus the opening width or against the ground temperature on a semi-log scale. The lines in Fig. 12 indicate the variations of convergence rates at given temperatures. Linear trends of Fig. 12 indicate that the convergence rate increases rapidly as ground temperature approaches thawing condition. Fig. 13 implies that for a given opening, every degree change in temperature influences the tunnel convergence rate by a factor of exp (1.15). From the data in Figs. 10 and 13, an increase of opening width at a given constant temperature does not cause a significant change in the convergence rate as the opening approaches a larger dimension. Thus the investigation data give evidence that temperature variations have more influence than roof span on tunnel stability in permafrost.

Fig. 14 shows the relationship between the overburden thickness and the average convergence rate of each monitoring station. As expected, the data indicates that the convergence rate increases as the overburden

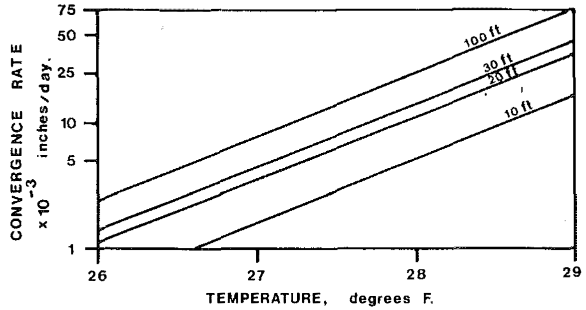

FIG. 13.—Plot of Eq. 4 Showing Relationship between Convergence Rate and Ground Temperature at Given Opening Width

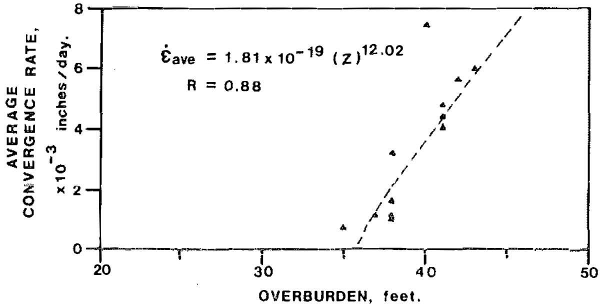

FIG. 14.—Average Convergence Rate versus Overburden Thickness (Correlation Coefficient = 0.88)

J. Geotech. Engrg., 1986, 112(8): 777-790

thickness increases. This trend, however, is less pronounced than the relationship of the opening width because of less variation in overburden thickness.

Due to the relatively uniform height along the tunnel, the analysis did not reveal any significant influence of tunnel height on the convergence rate.

Conclusions

An underground excavation in frozen silt will undergo continuous creep deformation. This continuous deformation is primarily temperature dependent. As the temperature of the ground surrounding the opening rises, the rate of deformation increases. The relationship between temperature and vertical convergence rate correlates to an exponential model. In addition to the effect of temperature, the overburden thickness and the opening width also have a direct effect on the convergence rate. The convergence rate does not increase linearly with an increase in tunnel width. The increase in the rate of convergence decreases exponentially with an increase in span length. Field measurements indicate that the overburden thickness shows an increasing convergence rate as the thickness of overlying sediment increases.

Acknowledgments

The writers gratefully acknowledge the U.S. Bureau of Mines for the support of this project. The writers also wish to thank Lucy Trant and Cathy Farmer for their assistance.

Appendix I.—References

1. Hartman, C. W., and Johnson, P. R., *Environmental Atlas of Alaska,* Univ. of Alaska, Fairbanks, Alaska, 1978, pp. 20–21.
2. Huang, S. L., "Temperature and Time Effects on the Closure of a Gravel Room in Permafrost," *Association of Engineering Geologists,* Vol. 22, No. 1, 1985, pp. 53–65.
3. Huang, S. L., and Wu, M. C., "In-Situ Displacement Analysis of Underground Opening in Permafrost Regions (II)—Time and Geometric Effects," *2nd Generic Mineral Technology Center Mine Systems Design and Ground Control Workshop,* November 12–13, 1984, Reno, Nev., pp. 73–84.
4. Huang, S. L., and Garbeil, H., "In-situ Displacement Analysis of Underground Opening in Permafrost Regions," *1st Generic Mineral Technology Center Mine Systems Design and Ground Control Workshop,* Nov. 28–29, 1983, Blacksburg, Va., pp. 67–83.
5. Pettibone, H. C., and Waddell, G., "Stability of an Underground Room in Frozen Gold Bearing Strata," *75th Annual Northwest Mining Assoc. Convention,* Dec. 5–6, 1969, Spokane, Wash.
6. Péwé, T. L., *Geologic Hazards of the Fairbanks Area, Alaska,* Division of Geological and Geophysical Surveys, Special Report 15, 1982, pp. 1–60.
7. Sellmann, P. V., *Geology of the USA CRREL Permafrost Tunnel, Fairbanks, Alaska,* U.S. Army Corps of Engineers Cold Regions Research and Engineering Laboratory Technical Report 199, USA CRREL, Hanover, N.H., 1967.
8. Thompson, E. G., and Sayles, F. H., "In-Situ Creep Analysis of a Room in Frozen Soil," *Journal of Soil Mechanics and Foundation Division,* ASCE, Vol. 18, No. SM4, Sept., 1972, pp. 899–914.

APPENDIX II.—NOTATION

The following symbols are used in this paper:

exp, e = 2.7183;
T = ground temperature;
W = unsupported roof span;
Z = overburden thickness;
$\dot{\epsilon}$ = convergence rate; and
$\dot{\epsilon}_{ave}$ = average convergence rate.

J. Geotech. Engrg., 1986, 112(8): 777-790